EXPERIMENTAL and MOLECULAR MEDICINE, Vol. 38, No. 6, 616-624, December 2006

Trichostatin A induces apoptosis in lung cancer cells *via* simultaneous activation of the death receptor-mediated and mitochondrial pathway

Hak-Ryul Kim[1], Eun-Jung Kim[2], Sei-Hoon Yang[1], Eun-Taik Jeong[1], Channy Park[2], Jae-Hyung Lee[2], Myung-Ja Youn[2], Hong-Seob So[2] and Raekil Park[2,3]

[1]Department of Internal Medicine
[2]Department of Microbiology
Wonkwang University School of Medicine
Jeonbuk 570-749, Korea
[3]Corresponding author: Tel, 82-63-850-6777;
Fax, 82-63-852-0220; E-mail, rkpark@wku.ac.kr

Accepted 29 September 2006

Abbreviations: HAT, histone acetyl transferases; HDAC, histone deacetylase; PARP, poly (ADP-ribose) polymerase; ICAD, inhibitor of caspase-activated deoxyribonuclease; MPT, mitochondrial membrane potential transition; TSA, trichostatin A

Abstract

Trichostatin A (TSA), originally developed as an antifungal agent, is one of potent histone deacetylase (HDAC) inhibitors, which are known to cause growth arrest and apoptosis induction of transformed cells, including urinary bladder, breast, prostate, ovary, and colon cancers. However, the effect of HDAC inhibitors on human non-small cell lung cancer cells is not clearly known yet. Herein, we demonstrated that treatment of TSA resulted in a significant decrease of the viability of H157 cells in a dose-dependent manner, which was revealed as apoptosis accompanying with nuclear fragmentation and an increase in sub-G_0/G_1 fraction. In addition, it induced the expression of Fas/FasL, which further triggered the activation of caspase-8. Catalytic activation of caspase-9 and decreased expression of anti-aptototic Bcl-2 and Bcl-X_L proteins were observed in TSA-treated cells. Catalytic activation of caspase-3 by TSA was further confirmed by cleavage of pro-caspase-3 and intracellular substrates, including poly (ADP-ribose) polymerase (PARP) and inhibitor of caspase-activated deoxyribonuclease (ICAD). In addition, a characteristic phenomenon of mitochondrial dysfunction, including mitochondrial membrane potential transition and release of mitochondrial cytochrome c into the cytosol was apparent in TSA-treated cells. Taken together, our data indicate that inhibition of HDAC by TSA induces the apoptosis of H157 cells through signaling cascade of Fas/FasL-mediated extrinsic and mitocondria-mediated intrinsic caspases pathway.

Keywords: apoptosis; histone deacetylases; lung neoplasms; trichostatin A

Introduction

Lung cancer is known to the leading cause of cancer death for both men and women although many of new therapeutic maneuvers have been developed in treatment of cancers (Jemal *et al*., 2004). The 5-yr survival for lung cancer patients with stage IIIa disease is 9-25% and stage IIIb disease only 3-7%. Thus, new therapeutic approaches in treatment of lung cancer are anxiously needed because the successful cure rate of treatment still remains very poor even though a number of newly developed agents have been clinically tried for decades (Schiller *et al*., 2002; Park *et al*., 2004).

Histones are small basic proteins which form the nucleosome core with DNA. A single nucleosomal core particle is composed of a fragment of DNA wrapped around a histone octamer composed by four histone partners, an H3-H4 tetramer and two H2A-H2B dimers (Luger *et al*., 1997). Post-translational modification of histones, including acetylation and methylation, results in changes of chromatin structure, which further allow the association or dissociation of transcriptional activators to promoter sites in the regulatory mechanism of various gene expression (Mei *et al*., 2004; Peterson *et al*., 2004; Monneret *et al*., 2005). Recent attention is focused in one of the two antagonist forms, acetylated or deacetylated histone residues. In this bidirectional enzymatic conversion, activation of histone acetyl transferases (HAT) results in the acetylation, which is also reversed by histone deacetylases (HDAC). Deacetylated histones are functionally contributed in cell growth, whereas hyperacetylated histones are responsible for cell growth arrest, differentiation, and

apoptosis (Marks *et al*., 2001). Therefore, it has been believed that uncontrolled regulation of HAT and HDAC activity serves a critical role in the tumorigenesis of certain human cancers by affecting the transcriptional patterns of many genes (Mahlknecht *et al*., 2000; Timmermann *et al*., 2001).

HDAC inhibitors, such as sodium n-butyrate, trapoxin, trichostatin A, depudecin, FR9011228, oxamflatin, and MS-27-275 (Cousens *et al*., 1979; Kijima *et al*., 1993; Hoshikawa *et al*., 1994; Kwon *et al*., 1998; Nakajima *et al*., 1998; Kim *et al*., 1999; Saito *et al*., 1999; Kim *et al*., 2005), induce the accumulation of acetylated histones in the nucleus. These compounds are known to cause growth arrest, differentiation, or apoptosis of transformed cells in culture (Marks *et al*., 2000). HDAC inhibitors also are responsible for the anti-proliferative activity and antitumor activity through selective induction of genes, which regulate the cell cycle and cell morphology (Han *et al*., 2000).

Trichostatin A (TSA), initially isolated as fungistatic antibiotics from *Streptomyces hygroscopicus* (Tsuji *et al*., 1979), is a potent inhibitor of HDAC activity at nanomolar concentrations. TSA has been suggested to block the catalytic reaction by chelating a zinc ion in the active site pocket through its hydroxamic acid group (Marks *et al*., 2001). Although TSA has been demonstrated to induce apoptosis of various cancer cells, but their effect on human non-small cell lung cancer cells is not clearly known yet. In this study, we evaluated the apoptotic potential of TSA in NCI-H157 human lung cancer cells and investigated the mechanism of TSA-induced apoptosis by analyzing the signaling pathway of apoptosis.

Materials and Methods

Reagents

RPMI 1640, fetal bovine serum (FBS), and antibiotics were obtained from GIBCO BRL Co. (Grand Island, NY). Trichostatin A (TSA), methylthiazol-2-yl-2,5-diphynyl, tetrazolium bromide (MTT), propidium iodide (PI), bicinchoninic acid (BCA), dimethyl sulfoxide (DMSA) were bought from Sigma Chemical Co. (St. Louis, MO). Antibodies against caspase-3, -8, -9, PARP, ICAD, FAS, FAS/L, Bax, Bid, Bcl-xL were purchased from Santa Cruz Biotechnology (Santa Cruz, CA). JC-1 was obtained from Molecular probes Co. (Eugene, OR) and antibody against anti-cytochrome c was bought from Pharmigen Co. (San Diego, CA). Anti-rabbit IgG conjugated with horseradish peroxidase antibody and enhanced chemiluminescent (ECL) kit were purchased from Amersham Pharmacia Biotech (Buckinghamshire, UK).

Cell culture and viability test

NCI-H157 human lung cancer cells were obtained from Korean Cell Line Bank (Seoul, Korea) and grown in RPMI 1640 containing 100 U/ml penicillin, 0.1 mg/ml streptomycin, and 10% FBS, and maintained in a humidified atmosphere of 5% CO_2 in air at 37°C and maintained in log phase. Cell viability was determined by MTT assay. Cells (5×10^4 /well) were seeded in 24 well plates and treated with TSA for the various concentrations. MTT (0.5 mg/ml) was added to 1 ml of cell suspension for 4 h. After three washes of cells with phosphate buffered saline (PBS, pH 7.4), the insoluble formazan product was dissolved in DMSO. Then, the optical density (OD) of each culture well was measured using Microplate reader (Titertek Multiskan, Flow Laboratories, North Ryde, Australia) at 590 nm. The OD of formazan formed in control cells was taken as 100% of viability and the positively stained cells with MTT were expressed as the percentage (%) compared to control cells.

Hoechst 33342 staining

H157 cells were fixed in PBS with 3.7% paraformaldehyde for 10 min, washed twice with PBS, and then incubated with 10 μM Hoechst 33342 (Sigma) in PBS at room temperature for 30 min. After incubation, cell morphology was observed under fluorescence microscope (Leica, Japan).

Flow cytometric analysis

Apoptosis was determined by measuring the number of cells showing below the G_0/G_1 phase of DNA content from Flow cytometric analysis after staining of cells with PI as originally described by Crissman and Steinkamp (1993). Cell cycle analysis was performed with FACScan equipped with a Cell Quest softwave (Becton Dickinson, San Jose, CA).

Caspase activity assay

To measure caspase activity, whole cell lysate was prepared in a lysis buffer as described previously and used to measure the catalytic activities of caspases (Kim *et al*., 2000). Cleavage of fluorogenic substrates, including 100 μM Ac-DEVD-AMC by caspase-3, Ac-IETD-AFC by caspase-8, and Ac-LEHD-AFC by caspase-9, was measured by spectrofluorometer (Jasco FR-777, Germany) at 380/460 nm, 405/505 nm, respectively.

Fluorescent staining of mitochondrial membrane potential transition (MPT)

H157 cells (10^7 cells/group) treated with TSA were harvested, washed with PBS, and then incubated

with 10 μg/ml JC-1 at 37°C for 30 min. After incubation, cell morphology was observed at 530 nm under fluorescence microscope (MPS 60, Leica).

Western blot analysis

Cell lysate was separated by 10% SDS-PAGE under reduced conditions and transferred onto nitrocellulose membrane. The membrane was blocked with 5% skim milk in TBS-T (25 mM Tris, pH 7.6, 138 mM NaCl and 0.05% Tween-20) for 1 h and probed with primary antibodies (1:1,000-1:5,000). After a series of washes, the membrane was further incubated with secondary antibody (1:2,000-1:10,000) conjugated with horse radish peroxidase (HRP). The immunoreactive signal was detected with enhanced chemiluminescent (ECL) detection system (Amersham Co, England).

Preparation of cytosolic and mitochondrial fractions

Preparation of cytosolic and mitochondrial fractions was performed according to the previous report (Wolf *et al*., 1999) with some modifications. In brief, H157 cells were harvested, washed with ice-cold PBS, and then incubated with 500 μM of buffer A (250 mM sucrose, 20 mM HEPES pH 7.5, 10 mM KCl, 1.5 mM $MgCl_2$, 1 mM EGTA, 1 mM EDTA, 1 mM DTT, 1 mM PMSF, 10 μg/ml each of leupeptin, aprotinin and pepstatin A) on ice for 30 min. Then, cells were disrupted by 20 passages through 26-gauge needle. The disrupted cells were centrifuged at 750 × *g* for 10 min. The supernatant was centrifuged at 10,000 × *g* for 25 min. After centrifugation, the cytosolic fraction was frozen at 70ºC. The pellet containing mitochondria was washed with ice-cold buffer A and then resuspended with cell lysis buffer. The resuspended pellet was incubated on ice for 30 min and then centrifuged at 10,000 × *g* for 25 min. The supernatant was collected as cytosolic fraction of H157 cells.

Statistical analysis

Each experiment was performed at least three times, and all values are represented as means ± SD of triplicates. Student's *t*-test was used to analyze a statistical significance of the results. Values of $P < 0.05$ were considered as statistically significant.

Results

Treatment with TSA decreased the viability of H157 cells with acetylation of histone isomers

To investigate whether TSA affects the viability of H157 cells, MTT assay was performed (Figure 1A).

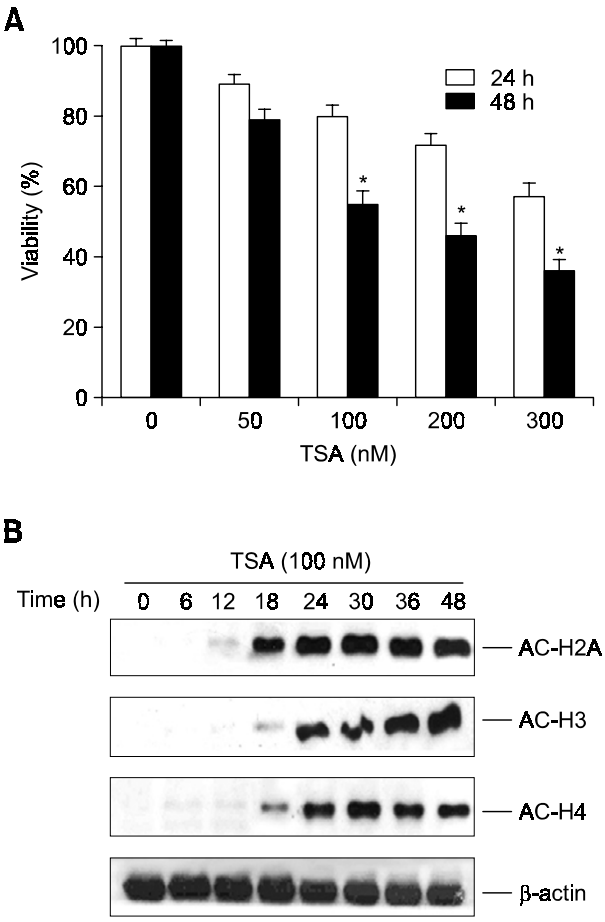

Figure 1. TSA treatment induced the decrease in cell viability and hyperacetylation of histones in H157 cells. (A) Cells were treated with various concentrations of TSA for up to 48 h. Viability was measured by MTT assay. The data represent the mean ± S.D. of three independent experiments. *$P < 0.05$ compared to control. (B) Lysate from cells treated with 100 nM TSA for 48 h was subjected to Western blotting with anti-acetylated histone H3, H4, and H2A antibodies.

Cells were treated with various concentrations of TSA for appointed period and cell viability was measured. Treatment with TSA resulted in a significant decrease in the viability of H157 cells in a dose-dependent fashion. Next, to determine the effects of TSA on the status of histone acetylation in H157 cells, cell lysate was used for Western blotting with anti-acetylated histone H2A, H3, and H4 antibodies (Figure 1B). Treatment with TSA increased the acetylation levels of histone isomers, including H2A, H3, and H4, in a time-dependent fashion at 18 h. Also, acetylation of H2A appeared earlier than other histone proteins at 12 h after treatment of 100 nM TSA.

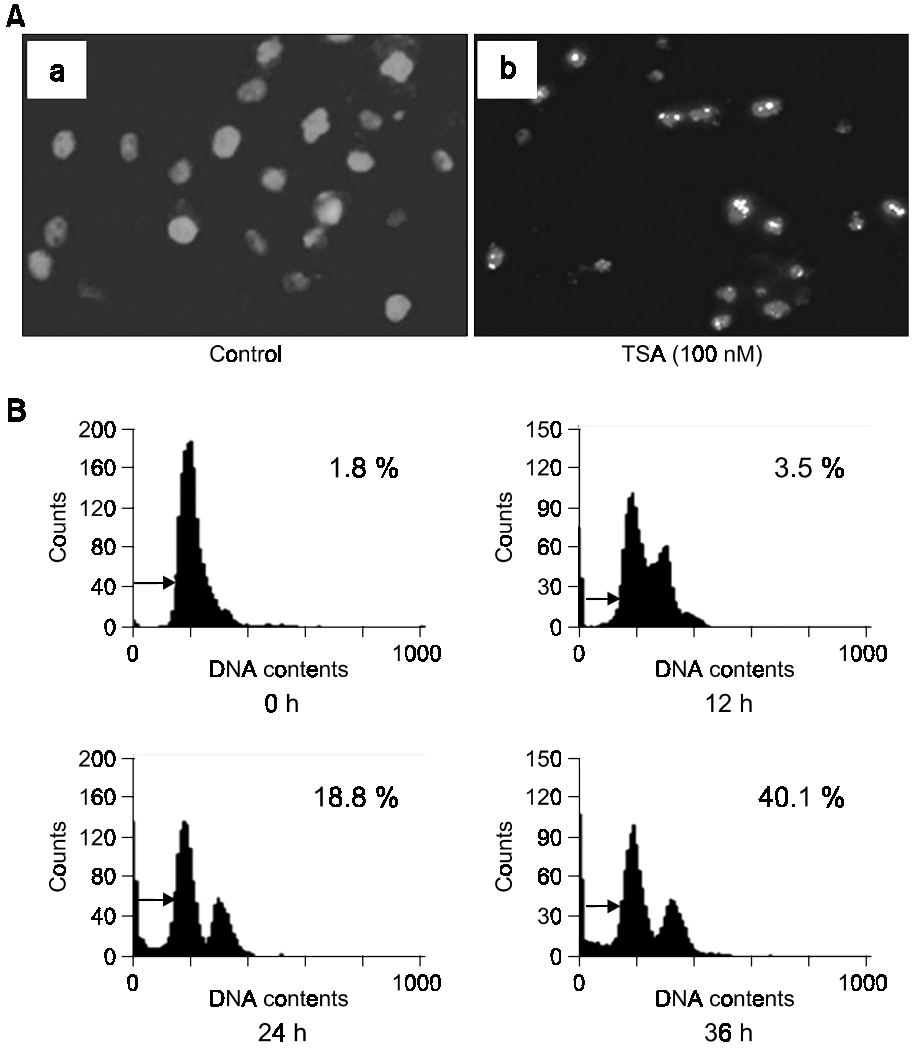

Figure 2. TSA treatment resulted in nuclear fragmentation and accumulation of sub- G_0/G_1 fraction in H157 cells. (A) Cells were treated with 100 nM TSA for 36 h, stained with Hoechst 33342 dye, and observed under fluorescent microscope; a) control, b) cells treated with TSA. (B) Cellular DNA was stained with PI and cell cycle was analyzed by flow cytometry. The data represent one of three independent experiments.

Treatment with TSA induced the apoptosis of H157 cells

To provide the nature of TSA cytotoxicity, the phenotypic characteristics of apoptosis were examined. Cells were treated with TSA for 36 h, stained with Hoechst dye 33342, and observed under fluorescent microscope (Figure 2A). Nuclei of control culture were oval round shape with homogenous intensity, whereas those of cells treated with TSA demonstrated as condensed and fragmented shape with irregularity in staining homogeneity. DNA fragmentation by TSA was further analyzed as the sub-G_0/G_1 fraction of cell cycle analysis by flow cytometry in H157 cells stained with PI (Figure 2B). Treatment with TSA markedly increased the accumulation of sub-G_0/G_1 fraction cells in a time-dependent manner. These data, collectively, indicate that TSA induces apoptotic death of H157 cells.

The catalytic activation of caspase-8 was occurred in TSA-treated H157 cells

The role of death receptor is well known in apoptosis of lung cancer cells after treatment with various chemotherapeutic agents (Fokkema *et al*., 2002). Thus, we first examined whether TSA affects the expression of Fas and FasL in H157 cells (Figure 3A). Cells were treated with 100 nM TSA for up to 48 h and lysate was used to carry out Western blot for Fas and FasL. The data revealed that treatment with TSA resulted in a marked increase in the expression of Fas and FasL proteins in a time-dependent fashion with the same kinetics. We, next, measured the catalytic activity of caspase-8, a downstream target of Fas/FasL, in cells treated with TSA for 48 h (Figure 3B). The catalytic activity of caspase-8 in TSA-treated cells started to increase at 24 h, reached a peak at 36-42 h, and gradually decreased in a time-dependent manner. Consistent with the

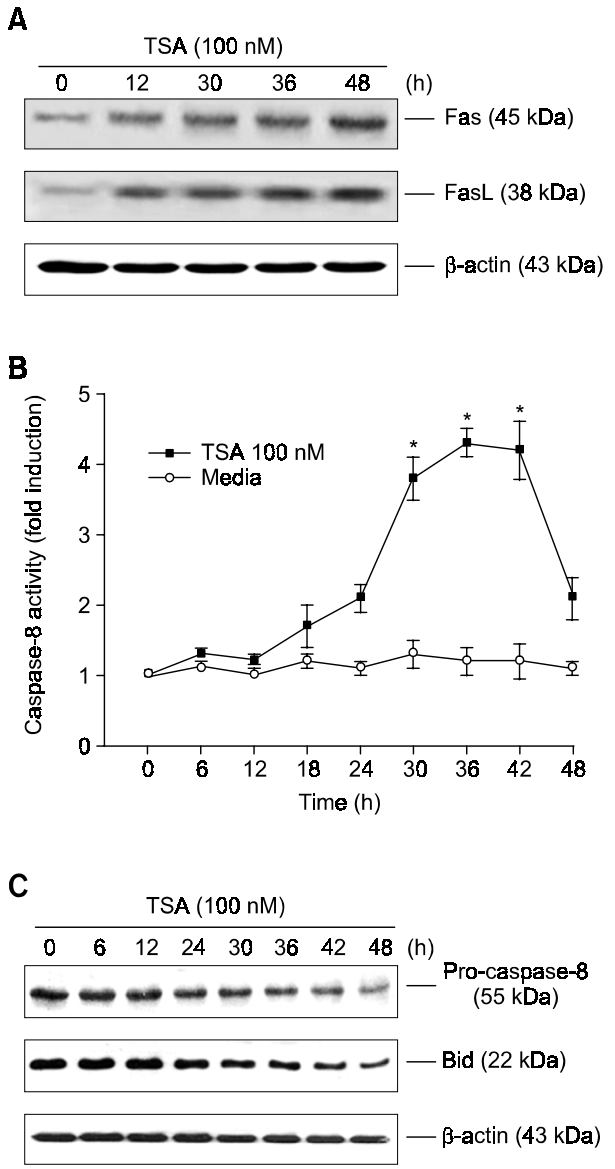

Figure 3. TSA treatment increased the expression of Fas/FasL and catalytic activity of caspase-8 in H157 cells. (A) Cells were treated with 100 nM TSA for 48 h and lysate was subjected to Western blotting with anti-Fas and anti-FasL antibodies. (B) lysate from cells treated with 100 nM TSA for up to 48 h was used to measure the catalytic activity of caspase-8 by using a fluorogenic substrate. $^*P < 0.05$. (C) Lysate was used to measure the expression of pro-caspase-8 and Bid protein by Western blotting.

catalytic activation, the expression level of pro-caspase-8 was going to decrease at 24 h after treatment with TSA (Figure 3C). These data indicate that treatment with TSA triggers to activate the extrinsic caspase pathway, including caspase-8 through Fas/FasL in H157 cells.

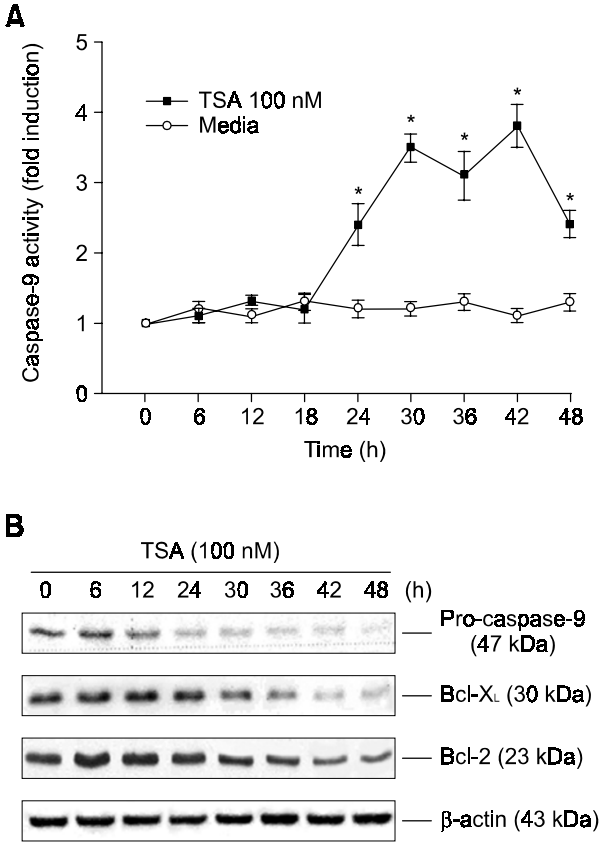

Figure 4. TSA treatment increased the catalytic activity of caspase-9 and decreased the expression of apoptogenic Bcl-X_L and Bcl-2 proteins in H157 cells. After treatment with 100 nM TSA for up to 48 h, lysate was used to measure the catalytic activity of caspase-9 by using a fluorogenic substrate (A) and subjected to Western blotting with anti-pro-caspase-9, anti-Bcl-X_L, and anti-Bcl-2 antibodies (B). $^*P < 0.05$.

The catalytic activation of caspase-9 and caspase-3 occurred in TSA-treated H157 cells

To confirm the implication of intrinsic caspase cascade, including caspase-9 and -3, cells were treated with 100 nM TSA and subjected to the *in vitro* catalytic activity assay for caspase-9 and -3. Similarly, caspase-9 was enzymatically activated at 24 h after TSA stimulation, reaches a maximum plateau for 30-42 h and gradually returned to the level of control cells (Figure 4A). We also confirmed that degradation of pro-caspase-9 was occurred by the addition of TSA in a time-dependent manner (Figure 4B, the first low). We further demonstrated that the expression level of anti-apoptotic Bcl-2 family proteins, including Bcl-X_L and Bcl-2, was time-dependently decreased in TSA-treated cells (Figure 4B, the second and third lows).

To gain the down-stream insights of activation of caspases, including caspase-8 and caspase-9, H157 cells were treated with 100 nM TSA for up to 48 h,

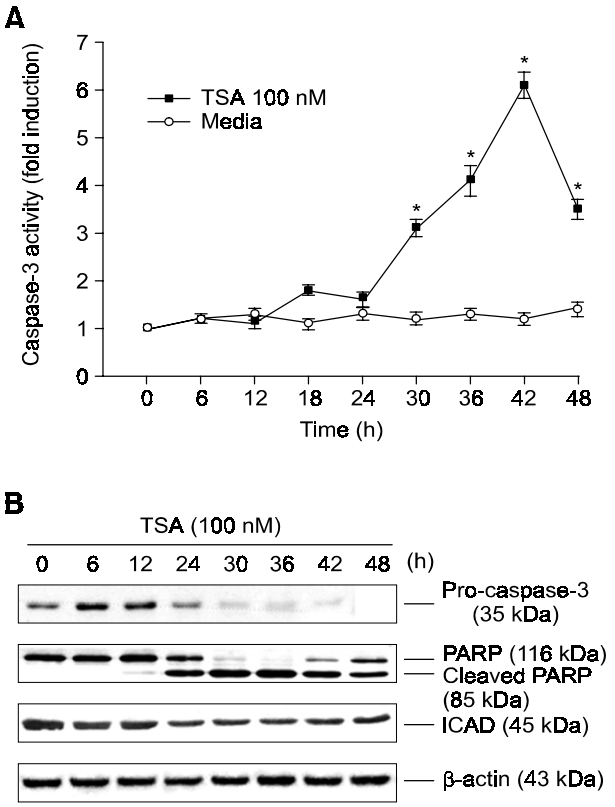

Figure 5. TSA treatment induced the activation of caspase-3 in H157 cells. After treatment with 100 nM TSA for up to 48 h, lysate was used to measure the catalytic activity of caspase-3 by using a fluorogenic substrate (A) and subjected to Western blotting with anti-pro-caspase-3, anti-PARP, and anti-ICAD (B). $^*P < 0.05$.

and the proteolytic activity of caspase-3 was determined (Figure 5A). The enzymatic activation of caspase-3 started after 30 h, attained its peak at 42 h, and sustained that level for 48 h in TSA-treated cells. To further confirm the activation of caspase-3, the cleavage of pro-caspase-3 and intracellular biosubstrates, including PARP and ICAD, was measured by Western blot analysis (Figure 5B). Degradation of pro-caspase-3 occurred at 24 h and the immunoreactive band was hardly detectible at 36 h after TSA treatment. Cleavage of PARP from 116 kDa to 85 kDa was clearly demonstrated at 24 h after TSA treatment. Also, ICAD expression was decreased by the addition of TSA in a time-dependent manner.

Treatment with TSA induced the mitochondrial dysfunction of H157 cells

To examine the up-stream event of caspase-3 in apoptosis signaling, markers of mitochondrial dysfunction, including mitochondrial membrane potential transition (MPT) and cytosolic release of cytochrome c, were evaluated in cells treated with TSA. Cells were treated with 100 nM TSA for 24 h and used to measure the MPT by staining mitochondria with JC-1 under fluorescence microscope (Figure 6A). Mitochondria were mainly located in cytosol as punctuated form colored with orange in control culture. Exposure of cells to TSA caused a dramatic change in MPT, shown as a diffuse form, and mainly located in the cytosol as well as nuclei. To provide further evidence of mitochondrial dysfunction, cytosolic release of cyto-

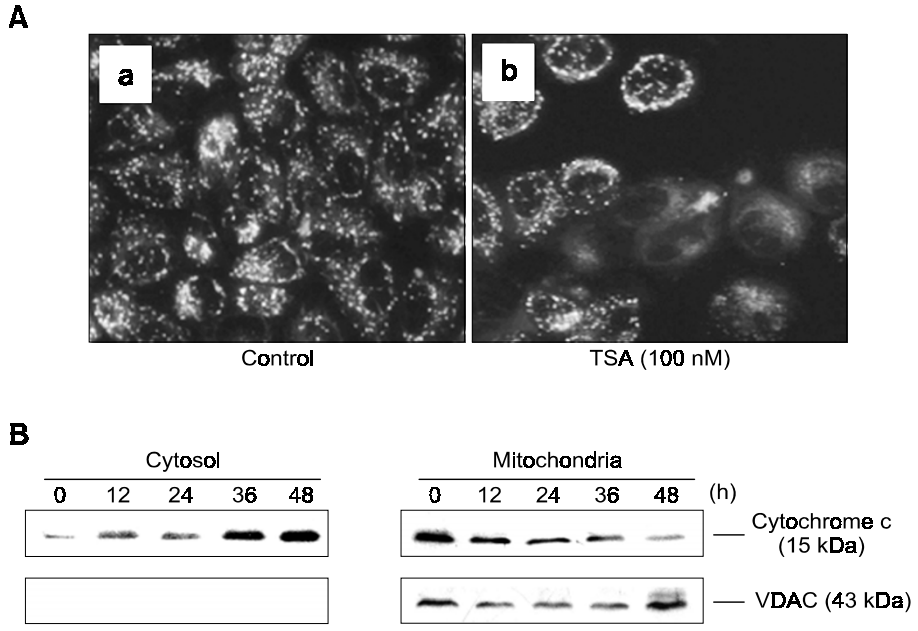

Figure 6. TSA treatment induced the mitochondrial dysfunction of H157 cells. (A) Cells were treated with 100 nM TSA for up to 24 h, stained with 10 μg/ml of JC-1, and observed under fluorescent microscope: a) control, b) cells treated with TSA. (B) Lysate from cells treated with 100 nM TSA for up to 48 h was fractionated into two parts, cytosolic and mitochondrial portions, and subjected to Western blotting with anti-cytochrome c antibody. The purity of mitochondrial fraction was determined by anti-VDAC antibody.

chrome c was examined by Western blot in both mitochondrial and cytosolic fractions (Figure 6B). Cytochrome c in cytosolic fraction was increased in a time-dependent fashion, correspondent with the decrease of cytochrome c in the mitochondrial fraction. The purity of mitochondrial fraction was verified by Western blot with anti-VDAC antibody. These results demonstrate that treatment with TSA activates apoptotic signaling through mitochondrial dysfunction, which further induces the catalytic activation of intrinsic caspase cascades.

Discussion

Histone acetylation is regulated by a balance between histone acetyltransferase (HAT) and histone deacetyltransferase (HDAC). It has been known to modulate the pattern of transcriptional expression by changing the dynamics of chromatin folding during gene expression (Grunstein *et al*., 1997). An inappropriate acetylation state of histones results in uncontrolled behaviors of proliferation and death of cells, which triggers neoplasmic transformation (Marks *et al*., 1978).

Inhibitors of HDAC induce apoptosis of many human cancer cell lines (Medina *et al*., 1997; Glick *et al*., 1999; Mandal *et al*., 1999). However, the mechanism by which HDAC inhibitors induce apoptosis is still not completely understood and includes activation of either caspase-dependent or caspase-independent pathways (Rosato *et al*., 2003). Apicidin causes the death of HL60 through *de nove* synthesis of Fas/Fas ligand and activation of the extrinsic/receptor mediated caspase pathway (Kwon *et al*., 2002). On the other hand, SAHA-induced mitochondrial disruption is involved in both reactive oxygen species (ROS) generation and cleavage of Bid, a BH3-only domain Bcl-2 family member (Ruefli *et al*., 2001).

TSA was originally isolated from the culture broth of *Streptomyces hygroscopicus* as an antifungal antibiotic and exhibits potent activities in differentiation and proliferation at nanomolar concentrations. Although TSA is reported to inhibit cell growth and induce apoptosis of various cancer cells (Roh *et al*., 2004; Yee *et al*., 2004), there is little evidence of its pharmacologic efficacy on lung cancer cells. Choi demonstrated that TSA induces apoptotic death of A549 lung cancer cell (Choi, 2005). Treatment of TSA results in a decrease in Bcl-2 expression, suppression of caspase activation, and a specific inhibition of COX-2 expression. Also, both inhibition of NF-κB and subsequent treatment with HDAC inhibitors, including TSA, potentiated apoptosis of lung cancer cells through a caspase-dependent mechanism (Mayo *et al*., 2003).

In our study, histone hyperacetylation in H157 cells by TSA was observed and persistent up to 48 h. The effect of TSA on the level of nuclear histone acetylation was closely correlated with cell death, which indicates that TSA-induced cell death was most likely due to inhibition of HDAC. Our data indicated that TSA-induced cell death is revealed as phenotypic characteristics of apoptosis, including nuclear fragmentation and accumulation of the sub-G_0/G_1 fraction.

To gain the mechanical insights of TSA-induced apoptosis, the catalytic activity of caspases and mitochondrial dysfunction were investigated in H157 cells. We herein demonstrated that TSA increased the enzymatic activity of intrinsic and extrinsic caspase cascades. Caspase-8, an initiator caspase, relays the apoptotic signal from death receptor of Fas/FasL, which further leads to cleavage of Bid (Li *et al*., 1998). In our experiment, both increase in Fas/FasL expression and the cleavage of Bid were observed in TSA-induced apoptosis of H157 cells. Therefore, the activation of caspase-8 was likely to be mediated by Fas and FasL. Furthermore, TSA also resulted in mitochondrial dysfunction evidenced by loss of mitochondrial membrane potential (MMP), changes in expression of Bcl-2 family proteins and cytosolic release of cytochrome c. Mitochondria are known as an important regulator of apoptosis (Green *et al*., 1998). It undergoes a series of consequent change during apoptotic death of cells. A loss of MMP together with the permeability transition of membrane pores is an early event in the apoptotic cascade and may sign of mitochondrial swelling and disruptions of the outer mitochondrial membrane (Vander Heiden *et al*., 1997). As a result of mitochondrial dysfunction, the cytosolic release of cytochrome c was occurred and it further contributes to activation of caspase-3, following activation of caspase-9. Consistently with previous reports in apoptosis signaling, our data demonstrated that TSA resulted in perturbation of mitochondrial functions in H157 cells.

In conclusion, we demonstrated that HDAC inhibitor TSA triggers apoptosis of H157 lung cancer cells *via* activation of the intrinsic caspase pathway along with Fas/FasL system and extrinsic caspase pathways along with mitochondrial dysfunction. Taken together, our data suggested that TSA may be practically useful in treatment of lung cancer.

Acknowledgement

This study was supported by grant of Wonkwang University in 2006.

References

Choi YH. Induction of apoptosis by trichostatin A, a histone deacetylase inhibitor, is associated with inhibition of cyclooxygenase-2 activity in human non-small cell lung cancer cells. Int J Oncol 2005;27:473-9

Cousens LS, Gallwitz D, Alberts BM. Different accessibilities in chromatin to histone acetylase. J Biol Chem 1979;254: 1716-23

Crissman HA, Steinkamp JA. Cell cycle-related changes in chromatin structure detected by flow cytometry using multiple DNA fluorochromes. Eur J Histochem 1993;37:129-38

Fokkema E, Groen HJ, Meijer C, Timens W, de Jong S, de Vries EG. The role of apoptosis-related genes in non-small-cell lung cancer. Clin Lung Cancer 2002;4:174-82

Glick RD, Swendeman SL, Coffey DC, Rifkind RA, Marks PA, Richon VM, La Quaglia MP. Hybrid polar histone deacetylase inhibitor induces apoptosis and CD95/CD95 ligand expression in human neuroblastoma. Cancer Res 1999;59: 4392-9

Green DR, Reed JC. Mitochondria and apoptosis. Science 1998;281:1309-12

Grunstein M. Histone acetylation in chromatin structure and transcription. Nature 1997;389:349-52

Han JW, Ahn SH, Park SH, Wang SY, Bae GU, Seo DW, Kwon HK, Hong S, Lee HY, Lee YW, Lee HW. Apicidin, a histone deacetylase inhibitor, inhibits proliferation of tumor cells *via* induction of p21WAF1/Cip1 and gelsolin. Cancer Res 2000; 60:6068-74

Hoshikawa Y, Kwon HJ, Yoshida M, Horinouchi S, Beppu T. Trichostatin A induces morphological changes and gelsolin expression by inhibiting histone deacetylase in human carcinoma cell lines. Exp Cell Res 1994;214:189-97

Jemal A, Tiwari RC, Murray T, Ghafoor A, Samuels A, Ward E, Feuer EJ, Thun MJ. Cancer statistics. CA Cancer J Clin 2004;54:8-29

Kijima M, Yoshida M, Sugita K, Horinouchi S, Beppu T. Trapoxin, an antitumor cyclic tetrapeptide, is an irreversible inhibitor of mammalian hisone deacetylase. J Biol Chem 1993;268:22429-35

Kim DH, Shim JS, Kwon HJ. Coordinated transcriptional regulation of calmegin, a testis-specific molecular chaperon, by histone deacetylase and CpG methyltransferase. Exp Mol Med 2005;37:492-6

Kim MS, So HS, Lee KM, Park JS, Lee JH, Moon SK, Ryu DG, Chung SY, Jung BH, Kim YK, Moon G, Park R. Activation of caspase cascades in Korean mistletoe (Viscum album var. coloratum) lectin-II-induced apoptosis of human myeloleukemic U937 cells. Gen Pharmacol 2000;34:349-55

Kim YB, Lee KH, Sugita K, Yoshida M, Horinouchi S. Oxamflatin is a novel antitumor compound that inhibits mammalian histone deacetylase. Oncogene 1999;18:2461-70

Kwon HJ, Owa T, Hassig CA, Shimada J, Schreiber SL. Depudecin induces morphological reversion of transformed fibroblasts *via* the inhibition of histone deacetylase. Proc Natl Acad Sci USA 1998;95:3356-61

Kwon SH, Ahn SH, Kim YK, Bae GU, Yoon JW, Hong S, Lee HY, Lee YW, Lee HW, Han JW. Apicidin, a histone deacetylase inhibitor, induces apoptosis and Fas/Fas ligand expression in human acute promyelocytic leukemia cells. J Biol Chem 2002;277:2073-80

Li H, Zhu H, Xu CJ, Yuan J. Cleavage of BID by caspase 8 mediates the mitochondrial damage in the Fas pathway of apoptosis. Cell 1998;94:491-501

Luger K, Mader AW, Richmond RK, Sargent DF, Richmond TJ. Crystal structure of the nucleosome core particle at 2.8 A resolution. Nature 1997;389:251-60

Mahlknecht U, Hoelzer D. Histone acetylation modifiers in the pathogenesis of malignant disease. Mol Med 2000;6:623-44

Mandal M, Adam L, Kumar R. Redistribution of activated caspase-3 to the nucleus during butyric acid-induced apoptosis. Biochem Biophys Res Commun 1999;260:775-80

Marks PA, Rifkind RA. Erythroleukemic differentiation. Annu Rev Biochem 1978;47:419-48

Marks PA, Richon VM, Rifkind RA. Histone deacetylase inhibitors: inducers of differentiation or apoptosis of transformed cells. J Natl Cancer Inst 2000;92:1210-6

Marks PA, Richon VM, Breslow R, Rifkind RA. Histone deacetylase inhibitors as new cancer drugs. Curr Opin Oncol 2001;13:477-83

Mayo MW, Denlinger CE, Broad RM, Yeung F, Reilly ET, Shi Y, Jones DR. Ineffectiveness of histone deacetylase inhibitors to induce apoptosis involves the transcriptional activation of NF-kappa B through the Akt pathway. J Biol Chem 2003; 278:18980-9

Medina V, Edmonds B, Young GP, James R, Appleton S, Zalewski PD. Induction of caspase-3 protease activity and apoptosis by butyrate and trichostatin A (inhibitors of histone deacetylase): dependence on protein synthesis and synergy with a mitochondrial/cytochrome c-dependent pathway. Cancer Res 1997;57:3697-707

Mei S, Ho AD, Mahlknecht U. Role of histone deacetylase inhibitors in the treatment of cancer. Int J Oncol 2004;25:1509-19

Monneret C. Histone deacetylase inhibitors. Eur J Med Chem 2005;40:1-13

Nakajima H, Kim YB, Terano H, Yoshida M, Horinouchi S. FR901228, a potent antitumor antibiotic, is a novel histone deacetylase inhibitor. Exp Cell Res 1998;241:126-33

Park HW, Song JY, Kim KS, Han Y, Kim CW, Yi SY, Yun YS. Enhancement of radiosensitivity by combined ceramide and dimethylsphingosine treatment in lung cancer cells. Exp Mol Med 2004;36:411-9

Peterson CL, Laniel MA. Histones and histone modifications. Curr Biol 2004;14:R546-51

Roh MS, Kim CW, Park BS, Kim GC, Jeong JH, Kwon HC, Suh DJ, Cho KH, Yee SB, Yoo YH. Mechanism of histone deacetylase inhibitor Trichostatin A induced apoptosis in human osteosarcoma cells. Apoptosis 2004;9:583-9

Rosato RR, Grant S. Histone deacetylase inhibitors in cancer therapy. Cancer Biol Ther 2003;2:30-7

Ruefli AA, Ausserlechner MJ, Bernhard D, Sutton VR, Tainton KM, Kofler R, Smyth MJ, Johnstone RW. The histone deacetylase inhibitor and chemotherapeutic agent suberoylanilide hydroxamic acid (SAHA) induces a cell-death pathway characterized by cleavage of Bid and production of reactive oxygen species. Proc Natl Acad Sci USA 2001;98:10833-8

Saito A, Yamashita T, Mariko Y, Nosaka Y, Tsuchiya K, Ando T, Suzuki T, Tsuruo T, Nakanishi O. A synthetic inhibitor of histone deactylase, MS-27-275, with marked *in vivo* antitumor activity against human tumors. Proc Natl Acad Sci USA 1999; 96:4592-7

Schiller JH, Harrington D, Belani CP, Langer C, Sandler A, Krook J, Zhu J, Johnson DH. Comparison of four chemotherapy regimens for advanced non-small-cell lung cancer. N Engl J Med 2002;346:92-8

Timmermann S, Lehrmann H, Polesskaya A, Harel-Bellan A. Histone acetylation and disease. Cell Mol Life Sci 2001;58: 728-36

Tsuji N, Kobayashi M, Nagashima K, Wakisaka Y, Koizumi K. A new antifungal antibiotic, trichostatin. J Antibiot 1979;29:1-6

Vander Heiden MG, Chandel NS, Williamson EK, Schumacker PT, Thomson CB. Bcl-xL regulates the membrane potential and volume homeostasis of mitochondria. Cell 1997;91: 627-37

Wolf CM, Eastman A. The temporal relationship between protein phosphatase, mitochondrial cytochrome c release, and caspase activation in apoptosis. Exp Cell Res 1999;247: 505-13

Yee SB, Kim MS, Baek SJ, Kim GC, Yoo KS, Yoo YH, Park BS. Trichostatin A induces apoptosis of p815 mastocytoma cells in histone acetylation-and mitochondria-dependent fashion. Int J Oncol 2004;25:1431-6